Available online at www.sciencedirect.com

ScienceDirect

Procedia Structural Integrity 5 (2017) 592–599

Structural Integrity Procedia

www.elsevier.com/locate/procedia

2nd International Conference on Structural Integrity, ICSI 2017, 4-7 September 2017, Funchal, Madeira, Portugal

Numerical analyses of corroded bolted connections

Zampieri Paolo[a]*, Andrea Curtarello[a], Emanuele Maiorana[b], Carlo Pellegrino[a]

[a]*Department of Civil, Environmental and Architectural Engineering, DICEA, University of Padova, Via Marzolo, 9 - 35131 Padova, Italy*
[b]*OMBA Impianti & Engineering SpA, Via della Croce 10 - 36040 Torri di Quartesolo, Italy*

Abstract

The interaction between fatigue and corrosion is the phenomena that is called Corrosion Fatigue (CF) and regarding steel structures subjected to cyclic loads. The S-N curves proposed by the main International Standards for fatigue life assessment do not take into account the state of degradation of the detail. For this reason, in this paper, a local approach is used to determine the fatigue life of corroded bolted joint with preload high strength bolts. In particular, fatigue life estimates are presented using the strain life method based on numerical analysis conducted on the joint, assuming that the crack nucleation phase is predominant in the whole fatigue life. The models used to simulate bolted joint are implemented using solid and contact elements and the geometry is realized taking into account the geometric imperfections produced by pitting corrosion. These imperfections were measured by surface surveys with a 3D profilometer. In conclusion, the results of the numerical analysis conducted on corroded joint model were compared with the experimental results obtained from cyclical tests.

Peer-review under responsibility of the Scientific Committee of ICSI 2017

Keywords: bolted connections, fatigue analysis, steel bridges, corrosion fatigue

1. Introduction

An important number of bolted bridges in the world require fatigue life assessment to allow their maintenance and retrofitting. In particular, steel structures exposed to atmospheric corrosion for long periods often exhibit high levels of surface corrosion, even if they are protected with superficial coating. Steel corrosion-related deteriorations,

* Corresponding author. Tel.: +39 049 827 5570; fax: +39 049 827 5570.
E-mail address: paolo.zampieri@dicea.unipd.it

2452-3216
Peer-review under responsibility of the Scientific Committee of ICSI 2017
10.1016/j.prostr.2017.07.020

including corrosion fatigue (CF), are the main contributors to the reductions of the structural integrity of metal bridges. Fatigue resistance can be significantly reduced by the presence of corrosion pitting because it facilitates the nucleation of the fatigue cracks at the pits propagating under cyclic loads.

The influence of corrosion is not only to be considered in terms of mass losses and corresponding reduction of the resistive area that are often negligible, but in the presence of superficial imperfections that generate stress concentrations defined notch factor effect (Rahgozar and Sharifi 2011). Also Zahrai (2003), Turnubull (2012) and Turnbull et al. (2010) concluded that fatigue life reduction is due to the irregularities that facilitate stress and strain concentrations and consequently cracks nucleation.

To assess the fatigue life taking into account the effect of surface imperfections one of the methodologies used is to model the geometry of the pits that are detected by a 3D measurements.

Sankaran et al.(2001) have conducted a research on the fatigue life of pre-corroded specimens using the shape of the pits to simulate elliptical cracks. Medved et al. (2004) modelled the pits through semi-elliptical geometry with shapes similar to the real ones. In the light of the results obtained by Shan-hua Xu and You-de Wang (2015), Xin-Yan Zhang et al. (2013) and M. Cerit et al. (2009) on unnotched specimens, the present study aim to obtain a fatigue life assessment of a fastened bolted connection subjected to accelerated corrosion through a finite element model based on surface detection of pits by means of a 3D profilometer. In this way, it was possible to analyse the fatigue behaviour taking into account surface pits effect. This methodology was pursued also by Athanasios Kolios et al. (2014) to study the effect of various typologies and numbers of pits.

The S-N curve obtained by numerical analysis were compared with the experimental data available for the case of study.

Nomenclature

f_y	Yield strength
f_u	Ultimate strength
N_f	Number of cycles to failure
N_i	Number of cycles for crack nucleation
N_p	Number of cycles for crack propagation
$\Delta\sigma$	Elastoplastic stress range
$\Delta\varepsilon$	Elastoplastic strain range
ΔS	Applied load range
E	Young module
K_t	Stress concentration factor
K'	Cyclic strength coefficient
n'	Cyclic hardening exponent
σ_f'	Fatigue strength coefficient
ε_f'	Strain ductility coefficient
b	Fatigue strength exponent
c	Strain ductility exponent
$F_{p,Cd}$	Bolt force pretension
f_{ub}	Bolt ultimate strength
A_s	Bolt net area
F_{normal}	Contact normal reaction force
K_{normal}	Contact stiffness
$x_{p.}$	Penetration
$F_{S,Rd}$	Joint force resistance
n	Number of friction resistant surfaces
n_b	Number of prel bolts
μ	Slip coefficient

2. Experimental procedure

2.1. Material and specimens

The structural detail studied is a slip resistant bolted joint made with using high strength preloaded bolts (Berto et al 2016). The plates are made of S355 structural steel with drilled holes and the overall geometry is shown in Figure 1. The chemical composition and mechanical properties of the steel used are reported in Table 1 and Table 2. Bolts are M12 class 10.9 with HR system. A tightening torque of 91Nm was applied during the assembly of the connection. The plates were treated with a SA3+ sandblasting.

Table 1. Chemical composition of S355 steel (wt.%).

C	Mn	Si	P	S	Cu	Ni	Cr	Nb
0.150	1.380	0.192	0.016	0.009	0.070	0.030	0.060	0.030

Table 2. Mechanical properties of S355 steel.

f_y (MPa)	f_u (MPa)
404	554

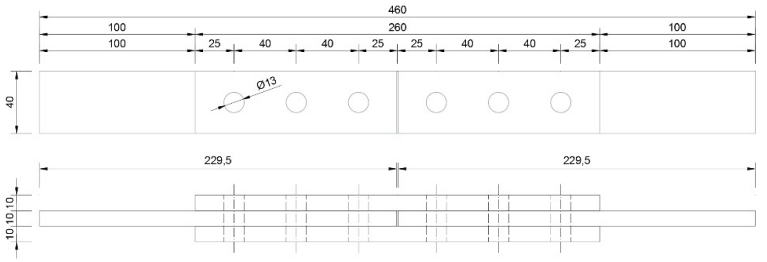

Fig. 1. Geometry of the bolted joints

2.2. Accelerated corrosion experiment

The accelerated corrosion process was conducted by referring to ISO 11130 (1999). The process consisted in submitting samples to alternating cycles of immersion and drying for the duration of 672h corresponding to 4 weeks. The cycles are characterized by 2min of immersion in a distilled water solution with 5% NaCl and by 60min of air exposure at the controlled temperature of about 35°C. Prior to initiating the accelerated corrosion process, samples were weighed with an electronic scale to be able to compare the mass losses caused by the oxidative phenomenon.

2.3. 2D and 3D surface profile measurements

Fig. 2. Position of the measured area

In order to characterize the specimens surfaces at the end of the corrosion process, roughness measurements were conducted using a Talysurf i-Series Taylor Hobson. The instrumentation used has a resolution of up to 0.4nm.

For each sample, the surface in which the specimen was assumed to be broken were measured; therefore the area was selected in the central plates along the thickness in correspondence of the outer bolts section. Sampling surfaces size were chosen in 5x5mm^2. A scheme of surface measurements is shown in Figure 2.

2.4. Fatigue test

Fatigue tests were conducted using the MTS810 servo-hydraulic system with a load capacity of 250kN. The frequency used to conduct tests was of 10Hz. The stress ratio value was set constant for all tests and equal to R = 0. All samples were subjected to cyclic loading tests at room temperature in laboratory air. Two sets of samples were subjected to cyclic tests: set A consisting of 8 not corroded specimens and set B consisting of 10 corroded specimens.

2.5. Fatigue model

Total fatigue life can be expressed as the number of cycles required for crack nucleation and the number of cycles necessary for its propagation as it can be seen in the following equation:

$$N_f = N_i + N_p \tag{1}$$

where N_f is the number of cycles to failure, N_i is the number of cycles forming a large crack (from 0.1 to 1 mm) and N_p is the number of cycles ranging from the formation of the crack to the breaking of the element. To estimate N_i in equation (1), strain-life equation can be used through the parameters of material obtained from fatigue tests on smooth specimens as proposed by the work of Abilio M.P. de Jesus et al. (2014). To describe N_p it is possible to use the theory of Linear Elastic Fracture Mechanics. In this paper, we investigate only the number of cycles required for the nucleation of the crack, as this is the term that most influences the fatigue life in the presence of low cyclic loads. The strain-life approach assumes that smooth specimens are subjected to cycling tests in which strain measurement are performed. The first relation used in the method is the Neuber (1961) equation (2) which correlates the elastic behaviour of the material to the real elastoplastic one. The proposed equation is:

$$\Delta\sigma\Delta\varepsilon = \frac{K_t^2 \Delta S}{E} \tag{2}$$

where $\Delta\sigma$ and $\Delta\varepsilon$ are respectively the elastoplastic stress range and elastoplastic strain range, ΔS is the applied load range, E is the young module and K_t is the stress concentration factor. To the describe elastoplastic behaviour from fatigue tests on smooth samples we use the Ramberg-Osgood (1943) relation (3):

$$\Delta\varepsilon = \frac{\Delta\sigma}{E} + 2\left(\frac{\Delta\sigma}{2K'}\right)^{1/n'} \tag{3}$$

where K' is the cyclic strength coefficient and n' is the cyclic hardening exponent. Finally, the relation that correlate strain and total cycles to failure takes the name of strain-life equation. In the present work we consider the one proposed by Smith, Watson and Topper (SWT) (4) to take into account the mean stress effect:

$$\sigma_{\max}\frac{\Delta\varepsilon}{2} = \frac{\left(\sigma_f'\right)^2}{E}\left(2N_f\right)^{2b} + \sigma_f'\varepsilon_f'\left(2N_f\right)^{b+c} \tag{4}$$

where σ'_f is the fatigue strength coefficient, ε'_f is the strain ductility coefficient, b is the fatigue strength exponent and c is the strain ductility exponent.

2.6. Procedure of the crack nucleation simulation and fatigue life assessment

The implementation of the approach described was conducted through the Fatigue Module proposed by the ANSYS Workbench software. The steps for fatigue analysis are summarized below:

- First step: defining the geometry of the connection, taking into account the surface imperfection detected by means of 3D profilometer in the case of corroded joint simulation;
- Second step: mesh generation, loads and constraints definition;
- Third step: linear elastic material analysis to achieve the stress concentration factor;
- Fourth step: input of the material characteristic parameters obtained from fatigue tests;
- Fifth step: setting cyclical parameters and detection of cycles corresponding to the loads applied in the FE analysis;

3. Finite element modelling of bolted joints

3.1. General aspects

The FE analysis were built on two different geometries using the ANSYS commercial code. The first geometry without imperfections was used to simulate the fatigue behaviour of the not corroded joint, the second one characterized by a notch comparable to the pits detected by superficial measurement was used to simulate the corroded samples. Models were designed taking into account a gap equal to 0.5mm between the surface of the plate holes and the bolts (bolt diameter of 12mm and hole diameter of 13mm used).

3.2. Simulation of the slip-resistant force

To simulate the friction effects on the joint behaviour a pretension force equal to that achieved by the tightening torque was applied to the bolts. The pretension force was calculated according to the EC3 prescriptions:

$$F_{p,Cd} = 0.7 \cdot f_{ub} \cdot A_s \tag{5}$$

where f_{ub} is the ultimate strength of the bolt and A_s is the net area of the bolt. The resulting force is equal to 59kN. This load was applied in a preliminary load step on the bolt shank along the local Z axis.

3.3. Finite element meshes, contacts, boundary conditions and material properties

The geometry was created modelling only half joint by exploiting the transversely symmetry. Because of the washer's fundamental role in the transmission of the pretension, it was decided to model also these parts. The geometry of the bolt shank was made without modelling thread. The model was constructed using tetrahedral elements with 10 node called SOLID187. These elements implement quadratic form functions. In Figure 3 it can be noted that the pit position was chosen at the inner plate and at the section of the outer bolt. In this position all samples were broken because of the decrease in the resistance net section and at the same time because of the high stress concentrations due to the large radius of the plate hole. Contacts formulation is based on the Pure Penalty theory:

$$F_{normal} = K_{normal} \cdot x_{penetration} \tag{6}$$

where K_{normal} represents the contact stiffness and $x_{penetration}$ represents the penetration. Specifically with regard to K the value 1.0 was used, for x the value 0.1 was used. Below the contacts used for model realization are reported:

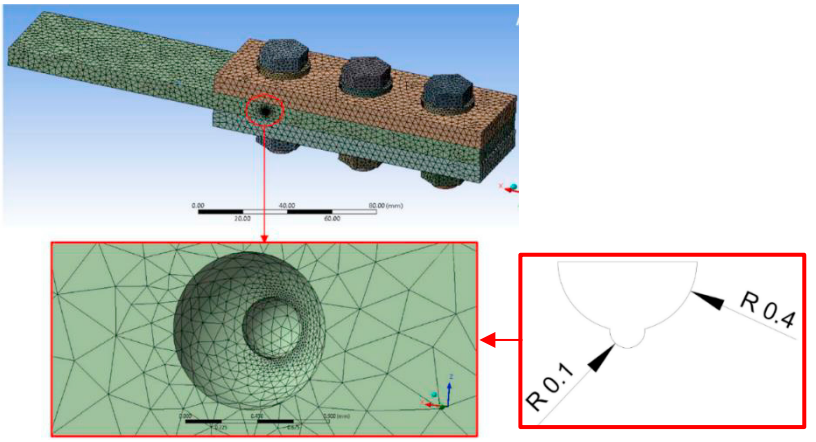

Fig. 3. Corroded meshed model.

- Bonded contact: it is used to tie two bodies between them, it is bilateral constraint both in the normal and in tangential direction. It was used to attach the bolt shank to the head and to the nut;
- Frictionless contact: it guarantees only a relative normal constraint; it is unilateral and needs a nonlinear solver. It was used to simulate the contact between the hole surface and the bolt shank surface;
- Frictional contact: it is a relative constraint both normal (one-sided) and tangential up to the friction limit that is set with the input of the slip coefficient value. It is unilateral and needs a nonlinear solver. It was used to model contact between plates with a slip coefficient equal to 0.5, and between bolt washers and head and bolt nut with a slip coefficient equal to 0.128.

The boundary conditions considered were the bolts preload and the fixed support to guarantee the symmetry constraint that were applied at the first analysis step. At the end of the first step, a linearly increasing force was applied to the inner plate along the X axis. The input data of the material are the ones that characterized a S355 steel with linear, elastic and isotropic properties (E=210000, ν=0.3). The analyses conducted were nonlinear due to contacts with nonlinear behaviour. The cyclic fatigue properties of the materials for the fatigue analysis conducted at the end of the FE analysis were the ones proposed by the work of Abilio M.P. de Jesus et al. (2012) and reported in Table 3.

Table 3. Stress-strain and strain-life cyclic parameters.

Material	K' (MPa)	n'	σ'_f(MPa)	b	ε'_f	c
S355	595.850	0.0757	952.200	-0.089	0.7371	-0.664

4. Numerical fatigue life assessment and comparison with experimental results

Prior to do the fatigue analyses a first analysis was conducted to verify the friction mechanism of the joint modelled.

To do this, we compare the friction resistance of the model with the analytical one. Thus, the force required to put bolts in contact with the hole surface was compared with the resistance of the joint calculated according to EC3:

$$F_{S,Rd} = n \cdot \mu \cdot F_{p,Cd} \cdot n_b \tag{7}$$

where n is the number of friction resistant surfaces (equal to 2), μ is the slip coefficient assumed equal to 0.5 and n_b is the number of bolts (equal to 3). From relation (7) there is a joint resistance of 177kN. To detect the joint sliding up to the loss of friction resistance, the gap size between the bolt shank and the inner hole surface was observed.

In Figure 4 it can be seen the gap pattern with the increasing of the imposed displacement. The gap initially equal to 0.5mm, reduces to zero in correspondence of a force equal to 172kN.

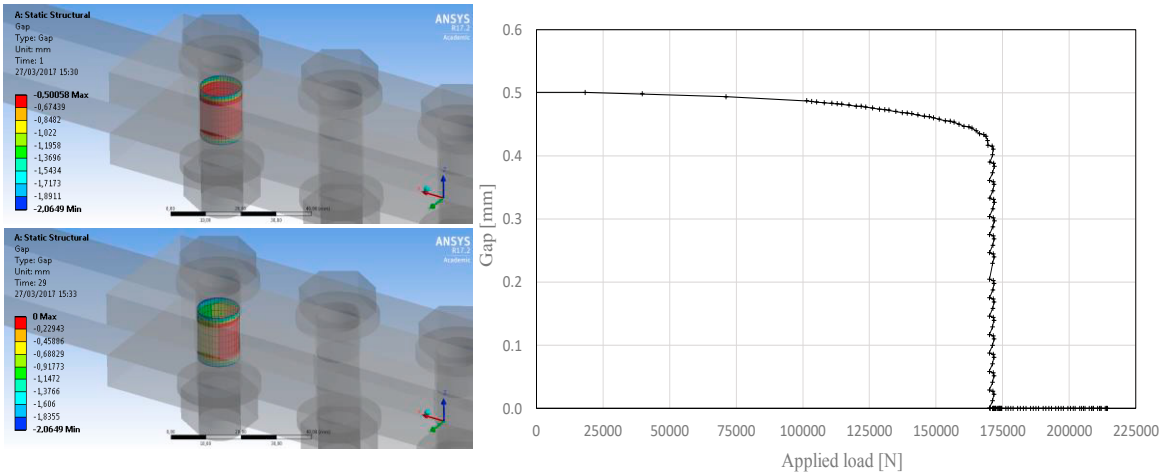

Fig. 4. Gap evolution along step increments

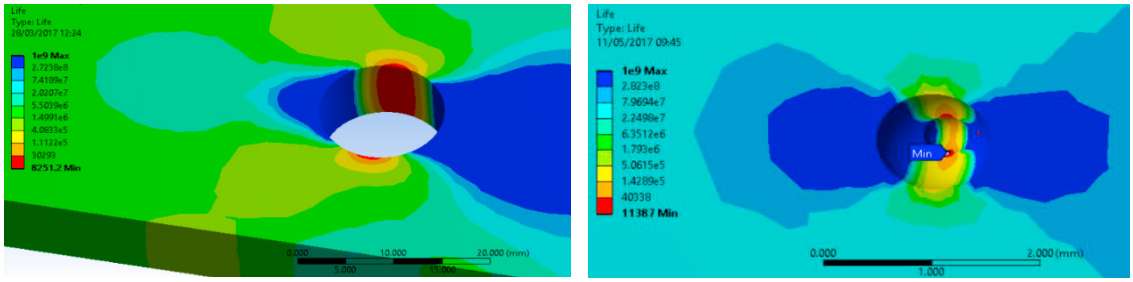

Fig. 5. Fatigue life contour: a) not corroded model; b) corroded model.

From FE analysis was possible to implement th Fatigue tool that gave the S-N curve for the two typologies of joint (corroded and not corrode). In Figure 5 it can be observed the fatigue life contours of the two models. In the case of not corroded connection, the lower fatigue life occurs at the outer hole of the central plate, where joints crack in the fatigue tests. For the corroded model, the minimum fatigue life is obtained at the imperfection introduced on the thickness of the central plate. This behaviour is caused by the presence of a smaller radius than that of the holes and consequently an increase in the stress concentration factor. In conclusion, the comparison between S-N experimental and numerical curve for corroded and not corroded joints are reported in Figure 6. The two arrows in the graphs indicate the samples that ran out, set over 2 million cycles. These values were not considered in the statistical processing of the experimental results for the construction of the S-N curves. In the graphs it can be seen how there is a good match between experimental and numerical S-N curve of not corroded joint, instead the S-N curves for corroded joints have much more pronounced difference.

5. Conclusions

In this paper the fatigue behaviour of a bolted connection with high strength bolts subjected to an accelerated corrosion process was investigated. The methodology presented was aimed to obtain the S-N curves by numerical analysis which was than compared with the experimental available results.

From the results of numerical analyses it was possible, through a strain life approach, to determine the fatigue life cycles of the studied joint. In order to introduce the corrosion effects into the numerical model, an imperfection comparable with the pits detected through 3D surface measurement was introduced at the critical crack position.

The comparison with the experimental data showed an expected correspondence for the model that simulates the behaviour of not corroded joint; a wide deviation emerged between the results of corroded joint. These results suggest

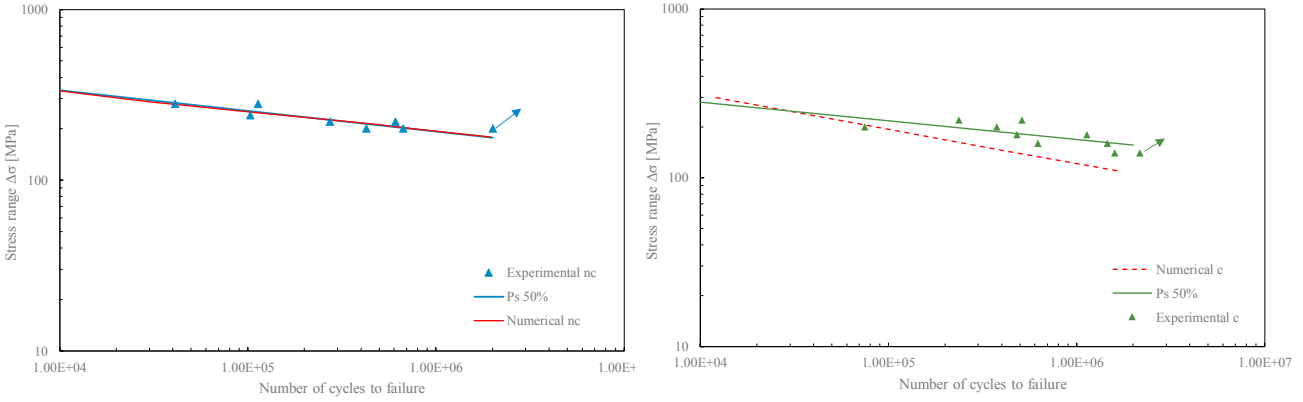

Fig. 6. Experimental and numerical results comparison: a) not corroded joints; b) corroded joints

that other factors may influence the decrease in fatigue resistance of the corroded connection, such as a variation in the slip coefficient between plates or a certain amount of loss of bolts pretension, which may resulted in a decrease in the friction resistance of the connection and consequently a bearing type behaviour of it.

Acknowledgements

The Author would thank to Prof. M. Quaresimin, Eng. N. De Rossi, Prof. G. Concheri and Eng. G. Savio for their technical support.

References

Rahgozar, R., Sharifi, Y. 2011. Remaining fatigue life of corroded steel structural members. Adv Struct Eng 14(5):881-90.
Zahrai, S.M. 2003. Cyclic strength and ductility of rusted steel members. Asian J Civil Eng (Build Housing) 4:135-48.
Turnbull, A. 2012. The environmentally small/short crack growth effect: current understanding. Corros Rev 30:1-17.
Turnbull, A., Wright, L., Crocker, L. 2010. New insight into the pit-to-crack transition from finite element analysis of the stress and strain distribution around a corrosion pit. Corrosion science 52:1492-1498.
Sankaran, K.K., Perez, R., Jata, K.V. 2001. Effect of pitting corrosion on the fatigue behavior of aluminum alloy 7075-T6: modeling and experimental studies. Mater Eng 297:223-9.
Medved, J.J., Breton, M., Irving, P.E. 2004. Corrosion pit size distributions and fatigue lives – a study of the EIFS technique for fatigue design on the presence of corrosion. International Journal of Fatigue 25:71-80.
Athanasios, K., Sumant, S., Konstantinos, S. 2014. Numerical simulation of material strength deterioration due to pitting corrosion. Procedia CIRP 13:230-236.
Shan-hua Xu, You-de Wang. 2015. Estimating the effects of corrosion pits on the fatigue life of steel plate based on the 3D profile. International Journal of Fatigue 72:27-41.
Xin-Yan Zhang, Shu-Xin Li, Rui Liang, R. Akid. 2013. Effect of corrosion pits on the fatigue life and crack initiation. 13th International Conference on Fracture, China.
Cerit, M., Genel, K., Eksi, S. 2009. Numerical investigation on stress concentration of corrosion pit. Engineering Failure Analysis 16:2467-2472.
Berto, F., Mutignani, F., Guido, E. 2016. Effect of hot dip galvanized on the fatigue behaviour of steel bolted connections. International Journal of Fatigue 93:168-172.
International Standard ISO 11130:1999. Corrosion of metals and alloys – Alternate immersion test in salt solution.
Abílio, M.P. de Jesus, António, L.L. da Silva, José, A.F.O. Correia. 2014. Fatigue of riveted and bolted joints made of puddle iron – A numerical approach. Journal of Constructional Steel Research 102:164-177.
Neuber, H. 1961. Theory of stress concentration for shear-strained prismatic bodies with arbitrary nonlinear stress-strain law. Translation of the ASME. J APPL Mech 28:544-50.
Ramberg, W., Osgood, W.R. 1943. Description of stress-strain curves by three parameters. Naca TN 402. National Advisory Committee for Aeronautics.
EN 1993-1-9:2005. Design of steel structures, Part 1-9: Fatigue.
Abílio, M.P. de Jesus, Rui, M., Bruno, F.C.F., Carlos, R., Luis Simões da Silva, Milan, V. 2012. A comparison of the fatigue behaviour between S355 and S690 steel grades. Journal of Constructional Steel Research 79:140-150.